Research article

advanced technologies

Received: 6 April 2014, Revised: 7 June 2014, Accepted: 26 August 2014, Published online in Wiley Online Library

(wileyonlinelibrary.com) DOI: 10.1002/pat.3404

"Experimentation and modeling for the apparent elongation viscosity of polymer melts with the White–Metzner model"

Gwo-Geng Lin*, Jin-Ton Chang and Ting-Wei Kuo

The measurement of the apparent elongation viscosity (η_e) of several polyolefin melts was conducted in this study by using the isothermal fiber-spinning method. The White–Metzner (W–M) model was used to analyze the spinning flow of the polymer melts and, thus, the elongation viscosity was predicted at elongation strain rates ranging from 0 to approximately 5 s^{-1}. The values of the model parameters required in the W–M model were obtained by curve fitting the experimental data obtained from the shear measurements. The elongation viscosity predicted using the W–M model was in good agreement with the experimental results of fiber spinning. In addition, η_e could also be estimated directly from the measured shear viscosity (η_S) with a formulation using the W–M model; the subsequently obtained elongation viscosity and Trouton ratio (T_R) were reasonable within a wide range of strain rates. Based on the experimental and theoretical results, the polyolefin with a high molecular weight was observed to have high elongation viscosity, and the polymer with a broad molecular weight distribution also possessed high η_e. The T_R value of the commercial polypropylene (PP-1040) began to increase from 3 at a deformation rate of 0.1 s^{-1} and grew up asymptotically to 10, whereas the T_R of high-density polyethylene (HDPE-606) remained nearly at 3 within the entire range of strain rates. Copyright © 2014 John Wiley & Sons, Ltd.

Keywords: elongational viscosity; fiber spinning; White-Metzner model; polyolefin; Trouton ratio

INTRODUCTION

Polymeric materials typically possess specific viscoelastic properties, which deeply affect the quality of the molded products during processing operations. For example, in general plastic processing, the residual stress can cause an undesirable part warpage. In manufacturing polymer optics such as CCD cameras, bar code scanners, motion sensors, and others, the flow-induced birefringence likely occurs in case of the bad part/mold design, or under poor processing conditions.[1,2] Among the aforementioned circumstances, the rheological properties of the polymer melt play a major role during the molding process. Furthermore, the molten polymeric materials might undergo stretching, because of the sudden contraction of the conduit cross section (e.g. near the die or gate in the injection molding), or in extensional processes such as fiber spinning, high-speed coating, cast-film extrusion, and blow molding. Therefore, studying the rheological behavior of polymeric melts under elongational conditions, which determine the quality of the molded product, is crucial. Polymer melts with similar shear-flow properties might differ in the response to elongation, indicating distinct processing characteristics. This means that considering the shear viscosity of polymer melts alone is not sufficient to characterize the processability of polymer materials from the viewpoint of the processing industry.

Relative to the rheological behavior demonstrated under shearing, the response of polymer melts to stretching (i.e. elongational deformation) is extremely complicated, and its accurate measurement is difficult. Ballman[3] developed the first uniaxial extension instrument and used it to stretch a molten polymer sample at a constant elongation rate by using an accelerating clamp. Meissner[4,5] devised an apparatus in which a filament is held horizontally between two pairs of rotating, tensioned rolls. Variations of this instrument have been described by other rheologists.[6–12] By using these homogeneous stretching methods, simple elongation flow was developed; thus, either the transient or the steady elongation viscosities for molten polymers can be obtained. The primary drawback of this Meissner-type rheometer is that the achievable experimental strain rate is extremely low, and the range of the strain rate is narrow.

Another valuable and convenient method for measuring the elongation viscosity of molten polymers is the fiber spinning.[13–18] Revenu *et al.* used this method to measure the transient elongation viscosity of polyethylene.[19] They photographically recorded the diameter of a polymer thread under spinning; both the strain rate and the tensile stress were then calculated using the mass and force balances, respectively, around the extended filament. Thus, the elongation viscosity of the extended polymer filament was obtained for the strain rate achieved. Cogswell[20,21] and Binding *et al.*[22,23] proposed a method to estimate the elongation viscosity at strain rates up to 10^2 s^{-1} by analyzing the shear and elongation components exhibited in the contraction flow. Barnes *et al.*[24]

* *Correspondence to: Gwo-Geng Lin, Department of Chemical and Materials Engineering, Energy and Opto-Electronic Materials Research Center, Tamkang University, Tamsui 25137, New Taipei City, Taiwan.*
E-mail: gglin@mail.tku.edu.tw

G.-G. Lin, J.-T. Chang, T.-W. Kuo
Department of Chemical and Materials EngineeringEnergy and Opto-Electronic Materials Research Center, Tamkang University, Tamsui, 25137, New Taipei City, Taiwan

reviewed experimental methods for measuring elongation viscosity, such as homogeneous stretching using various types of constant stress or strain rate, fiber spinning, lubricated flows, contraction flows, and an open-syphon method. White[25] also reviewed the instruments used for elongational rheometry, including uniaxial, biaxial, and planar extensions.

A number of rheological models have been proposed to describe the rheological behaviors of polymeric liquids undergoing various types of deformations. The Wagner, White–Metzner (W–M), KBKZ (developed by Kaye, Bernstein, Kearsley, and Zapas), and Larson models have been extensively used to describe the viscoelastic properties of polymer melts.[26–31] For polyolefins such as low-density polyethylene (LDPE) and linear low-density polyethylene (LLDPE), the Wagner model can be used to successfully quantify the first normal stress difference (N_1) and the steady shear viscosity (η_s). The W–M model, which is a simple nonlinear, single relaxation-time model, was used to simultaneously predict both shear and elongational viscosity as a function of the deformation rate by Barnes *et al.*[29] The KBKZ model can be used to determine the influence of viscous dissipation and heating on flow properties by using an entropic constitutive equation. The Larson model has been commonly used to describe the viscoelastic behaviors of molten linear polymers. Recently, Lin *et al.*[32] reported that the Larson model along with rheological measurements can be applied to estimate both elongation and shear viscosities, and the normal stress of polyolefin melts. In our previous study,[33] the Phan–Thien–Tanner (PTT) constitutive equation along with a material parameter, called the slip constant, was used to model the elongation viscosity, which was agreeable with the measured data.

In this study, the W–M model was used to model the uniaxial elongational flow of molten polyolefins; thus, the *theoretical* elongation viscosity was obtained. In addition, the experimental data was *measured* using the fiber-spinning method developed in our previous study.[34] The Rheotens (Gottfert tensiometer) device was used to determine the drawdown force of the extruded polymer melts, which were extended using a pair of clamped rollers located downstream. Thus, a steady-state uniaxial extensional flow was attained, and the computations for determining the elongation viscosity that were conducted following the approach proposed by Revenu *et al.*[19]

Theoretical

Prediction of elongation viscosity by using the W–M model

On the basis of the formulation presented by Minoshima *et al.*[18] for the melt spinning, the W–M model was employed to estimate the extensional viscosity of the polymer melt, and the required model parameters were obtained by curve fitting the viscometric data. Written in tensorial form, the White–Metzner equations can be represented as:

$$\underset{\approx}{\sigma} = -p\,\underset{\approx}{I} + \underset{\approx}{\tau} \tag{1}$$

$$\lambda\frac{\delta\underset{\approx}{\tau}}{\delta t} = 2G\lambda\,\underset{\approx}{d} - \underset{\approx}{\tau} \tag{2}$$

$$\lambda = \frac{\lambda_0}{1 + a\lambda_0 II_d}, \left(II_d = \sqrt{2trd^2}\right) \tag{3}$$

$$\frac{\delta\underset{\approx}{\tau}}{\delta t} = \frac{\partial\underset{\approx}{\tau}}{\partial t} + \left(\underset{\sim}{v}\cdot\underset{\sim}{\nabla}\right)\underset{\approx}{\tau} - \underset{\sim}{\nabla}\underset{\sim}{v}^T\cdot\underset{\approx}{\tau} - \underset{\approx}{\tau}\cdot\underset{\sim}{\nabla}\underset{\sim}{v} \tag{4}$$

where $\underset{\approx}{\sigma}$, $\underset{\approx}{\tau}$, and $\underset{\approx}{I}$ are the total stress tensor, extra stress tensor, and unit tensor, respectively; p, G , λ, and λ_0 are pressure, shear modulus, relaxation time, and relaxation time at a zero-shear rate, respectively; "a" in eqn (3) and $\underset{\approx}{d}$ are the material constant, called the softening number, and the rate of deformation tensor, respectively; II_d is the second invariant of the rate of deformation tensor, $\delta/\delta t$ denotes the upper-convected time derivative, and $\underset{\sim}{\nabla}\underset{\sim}{v}$ is the velocity gradient.

By applying the W–M model to analyze the fiber-spinning flow, the formula for calculating the apparent elongation viscosity can be derived as follows. The uniaxially elongational flow is obtained using

$$v_1 = v_1(x_1) = \dot{\varepsilon}\cdot x_1 \tag{5}$$

$$v_2(x_2) = v_3(x_3) = -\frac{1}{2}\dot{\varepsilon}\cdot x_2 = -\frac{1}{2}\dot{\varepsilon}\cdot x_3 \tag{6}$$

The constant tensile force, F, exerted on the elongated polymer thread by the pair of clamping rollers is[35]

$$F = \sigma_{11}\pi R^2 = (\tau_{11} - \tau_{22})\pi R^2 = (\tau_{11} - \tau_{22})\frac{Q}{v_1} \tag{7}$$

The stress and rate of deformation tensors then become

$$\underset{\approx}{\tau} = \begin{pmatrix} \tau_{11} & 0 & 0 \\ 0 & \tau_{22} & 0 \\ 0 & 0 & \tau_{33} \end{pmatrix}, \underset{\approx}{d} = \begin{pmatrix} \dot{\varepsilon} & 0 & 0 \\ 0 & -\frac{1}{2}\dot{\varepsilon} & 0 \\ 0 & 0 & -\frac{1}{2}\dot{\varepsilon} \end{pmatrix}$$

and the upper-convected time derivative of the stress tensor is

$$\frac{\delta\underset{\approx}{\tau}}{\delta t} = \begin{pmatrix} \frac{\partial\tau_{11}}{\partial t} & 0 & 0 \\ 0 & \frac{\partial\tau_{22}}{\partial t} & 0 \\ 0 & 0 & \frac{\partial\tau_{33}}{\partial t} \end{pmatrix} + \begin{pmatrix} v_1\frac{\partial\tau_{11}}{\partial x_1} & 0 & 0 \\ 0 & v_1\frac{\partial\tau_{22}}{\partial x_1} & 0 \\ 0 & 0 & v_1\frac{\partial\tau_{33}}{\partial x_1} \end{pmatrix} - \begin{pmatrix} 2\tau_{11}\dot{\varepsilon} & 0 & 0 \\ 0 & -\tau_{22}\dot{\varepsilon} & 0 \\ 0 & 0 & -\tau_{33}\dot{\varepsilon} \end{pmatrix}$$

Therefore, at steady state, the component forms of tensorial eqn (2) can be written as

$$\lambda\left(v_1\frac{\partial\tau_{11}}{\partial x_1} - 2\tau_{11}\frac{\partial v_1}{\partial x_1}\right) = 2G\lambda\frac{\partial v_1}{\partial x_1} - \tau_{11} \tag{8.a}$$

$$\lambda\left(v_1\frac{\partial\tau_{22}}{\partial x_1} + \tau_{22}\frac{\partial v_1}{\partial x_1}\right) = -G\lambda\frac{\partial v_1}{\partial x_1} - \tau_{22} \tag{8.b}$$

and subtracting eqn (8.b) from eqn (8.a) gives

$$\lambda\left(v_1\frac{d}{dx_1}\frac{Fv_1}{Q} - 2\frac{Fv_1}{Q}\frac{dv_1}{dx_1}\right) = 3G\lambda\frac{dv_1}{dx_1} - \frac{Fv_1}{Q} + 3\tau_{22}\lambda\frac{dv_1}{dx_1} \tag{9}$$

Therefore,

$$\frac{F}{Q}\left(\frac{1}{\lambda} - \frac{dv_1}{dx_1}\right) = 3(G + \tau_{22})\frac{dv_1}{dx_1}\frac{1}{v_1} \tag{10}$$

polymers advanced technologies

and inserting eqn (3) into eqn (9) gives

$$\eta_e = \frac{\sigma_{11}}{\frac{dv_1}{dx_1}} = \frac{3(G+\tau_{22})\lambda_0}{1+\left(\sqrt{3}\,a-1\right)\lambda_0\frac{dv_1}{dx_1}} \tag{11}$$

The normal stress τ_{22} is well known to be very small, so we can assume $G \gg \tau_{22}$, and then the formula for computing the apparent elongation viscosity can be obtained as follows (eqns (12)):

$$\eta_e = \frac{3G\lambda_0}{1+\left(\sqrt{3}\,a-1\right)\lambda_0\frac{dv_1}{dx_1}} = \frac{3\eta_0}{1+\left(\sqrt{3}\,a-1\right)\lambda_0\frac{dv_1}{dx_1}} \tag{12}$$

The shear modulus, G, was determined by curve-fitting the relation between the first normal stress difference, N_1, and the shear stress, τ_{12}, in a steady shear flow,

$$N_1 = 2\tau_{12}^2/G \tag{13}$$

The λ_0 value was obtained from the zero shear viscosity (eqn (14)):

$$\lambda_0 = \eta_0/G \tag{14}$$

and the "a" parameter was obtained from the best fits of the shear viscosity $\eta_S(\dot{\gamma})$ as a function of shear rates.

Calculation of η_e using shear viscosity coupled with the W–M model

By introducing the cross-type representation of the relaxation time, eqn (3), in the W–M model, Barnes *et al.*[29] developed the following expression for extensional viscosity:

$$\eta_e = \frac{2\eta_s(II_d)}{\left(1-\frac{2}{\sqrt{3}}\lambda(II_d)II_d\right)} + \frac{\eta_s(II_d)}{\left(1+\frac{1}{\sqrt{3}}\lambda(II_d)II_d\right)} \tag{15}$$

where η_S is the steady shear viscosity and was obtained experimentally in this work.

Regarding simple shear flow, the second invariant of the rate of deformation tensor (II_d) is $\dot{\gamma}$, and it is $\sqrt{3}\,\dot{\varepsilon}$ for simple elongation flow. Applying eqn (15) to predict η_e by using the viscometric data of the shear flow is extremely convenient.

Experimental

In this study, the rheological measurements were conducted on the following commercial polyolefins: low-density polyethylene (LDPE), high-density polyethylene (HDPE), and polypropylene (PP). The molecular characteristics of these polyolefins are listed in Table 1.

Fiber-spinning method

The elongation viscosity at strain rates ranging from 0.2 to approximately 4 s^{-1} was measured by applying the fiber spinning method,[34] using a Rheotens (Gottfert tensiometer) device. The aforementioned polyolefin pellets were melted in an extruder equipped with a 20-mm ϕ screw and extruded through an orifice. The molten thread was then uniaxially extended by being clamped with a pair of rollers located 19 cm downward from the orifice, and the tensile force required to pull the melt was detected and recorded using the tensiometer. A heating chamber was designed and installed around the extended filament to maintain a constant temperature. Thus, the relationship between the elongation viscosity and the strain rate could be evaluated according to the method proposed by Revenu *et al.*[19] As reported in Ref.[34], the maximal elongation rate which can be achieved was restricted by the occurrence of the draw resonance and the breaking of the polymer melt. It should be noted that η_e measured by using the fiber spinning is merely the "apparent" elongation viscosity because of the non-homogeneous strain rates along the whole extended thread. The temperature shifting factor (a_T), defined as the ratio of the zero-shear-rate viscosity at temperature T to its value at the reference temperature T_0 as follows,

$$a_T = \frac{\eta_0(T)}{\eta_0(T_0)} \tag{16}$$

was used to obtain the master curve of the extensional viscosity.

Measurements using a rheometer

To facilitate the comparisons between the elongation and shear viscosities and to evaluate the material parameters in the W–M model, shear viscosity and primary normal stress were measured using a rotational rheometer (Rheometrics Dynamic Analyzer, Model RDA-II, Rheometrics Inc., USA) at low shear rates, and the high shear-rate viscosity was measured using a capillary rheometer (Rosand Rheometer RH-720, Rosand Precision Ltd., USA). The instrumental data obtained from these viscometric measurements were used in determining the model parameters with the curve-fitting method, the results of which are listed in Table 2. As stated in the section "Theoretical" with eqn (13), the shear modulus, G, in the W–M model can be curve fitted from the relation between the first normal stress difference and the squared shear stress in a steady shear flow, as shown in Fig. 1 for the sample of PP-1040 at 180°C. It was found that, at shear rates below 1.58 s^{-1}, the relationship behaves as a straight line with a slope equal to $G/2$.

Table 1. The molecular characteristics of the polyolefins used in this study

Material	Manufacturer	$\overline{M}w$	$\overline{M}n$	*MWD*	*MI*[a]	Notes[b]
PP-1040	Yung Chia Chem. Ind. Co., Taiwan	4.05E5	4.1E4	9.89	3.63	Yarn grade
PP-1080	Yung Chia Chem. Ind. Co., Taiwan	1.52E5	3.04E4	4.94	11.0	Injection grade
PP-2080	Yung Chia Chem. Ind. Co., Taiwan	2.50E5	3.12E4	8.03	10.93	Used for inflation film
HDPE-606	USI Far East Co., Taiwan	1.16E5	1.66E4	6.98	5.46	Injection grade
HDPE-405	USI Far East Co., Taiwan	1.19E5	1.87E4	6.36	5.91	
HDPE-614	USI Far East Co., Taiwan	9.96E4	1.27E4	7.82	10.55	
LDPE-207	USI Far East Co., Taiwan	2.64E5	2.64E4	9.97	8.0	Film-blowing
LDPE-208	USI Far East Co., Taiwan	2.04E5	2.29E4	8.92	22.0	Injection grade

[a]: Testing condition(ASTM D-1238):
HDPE, 190°C/2.16 kg; PP, 230°C/2.16 kg.
[b]: From the manufacturer's data sheet.

Table 2. The material parameters in the White–Metzner model

Material	Temp (°C)	a	λ_0 (sec)	η_0 (Pa*s)
PP-1040	180	0.640	3.094	17,648
PP-1040	200	0.705	1.368	9,225
PP-1040	220	0.720	0.947	4,556
PP-1080	180	0.856	1.210	7,511
PP-1080	200	0.857	1.312	5,009
PP-1080	220	0.893	0.889	3,661
PP-2080	180	0.905	1.179	6,016
PP-2080	200	1.058	0.396	3,120
PP-2080	220	0.920	0.338	1,870
HDPE-405	180	1.221	0.061	1,436
HDPE-606	180	1.118	0.077	1,599
HDPE-614	180	1.123	0.050	900

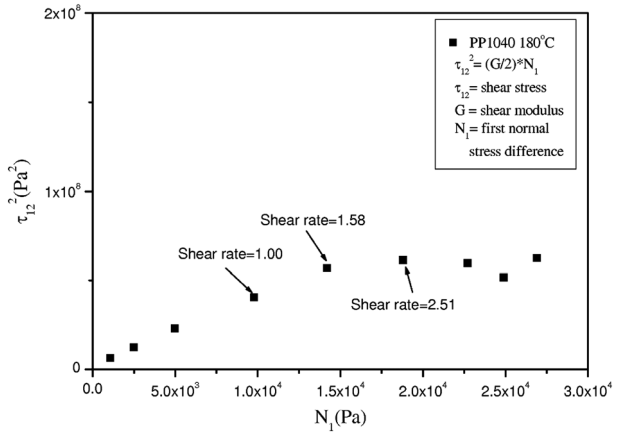

Figure 1. Squared shear stress versus first normal stress difference in steady shear flow for PP-1040 at 180°C.

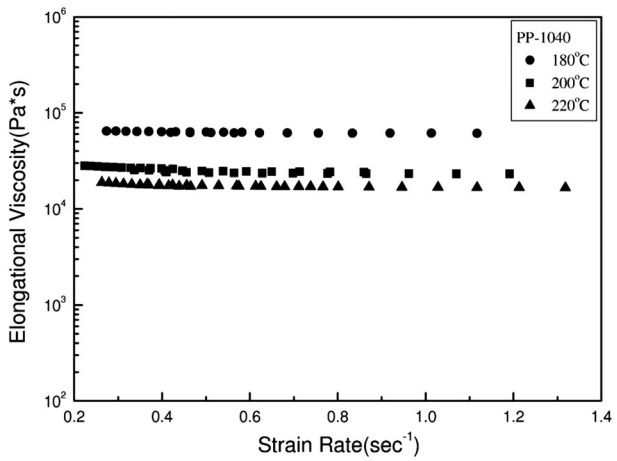

Figure 2. Elongation viscosity versus strain rate of PP-1040 measured under various testing temperatures.

RESULTS AND DISCUSSIONS

Figure 2 shows the elongational viscosity as a function of strain rate $(\dot{\varepsilon})$ for PP-1040, measured at various temperatures using the fiber spinning method. An increase in η_e was observed as the temperature decreased. In addition, within a small range of attained strain rates, η_e did not depend on $\dot{\varepsilon}$. Figure 3 shows the elongational viscosity versus $\dot{\varepsilon}$ plots for the three types of PP, measured at 220°C. The elongation viscosity of PP-1040 was higher than that of PP-1080 because of the effect of MW. However, the low viscosity of PP-2080 can be attributed to the addition of lubricants used for causing anti-blocking and slipping effects in the film-blowing process. Figure 4 shows the η_e versus $\dot{\varepsilon}$ plots for the three types of HDPE measured at 180°C. These plots indicate that a high elongation viscosity was related to high MW. Regarding the polymers with a similar average molecular weight, the polymer with a broad molecular weight distribution (i.e. high MWD) exhibited high elongation viscosity, as shown in Fig. 4, for HDPE-606 and HDPE-405. HDPE-606 had a high MWD and thus high η_e relative to HDPE-405, although both have a similar molecular weight. The effect of MW on elongation viscosity was also illustrated in Fig. 5 for LDPE.

The extension–viscosity master curve of PP-1040 at the reference temperature of 220°C is shown in Fig. 6, where the shifting factor (a_T) at temperature T was computed using eqn (16). At low strain rates achieved by the fiber spinning in this study, the experimental η_e versus $\dot{\varepsilon}$ were aligned approximately in a straight line, independent of the temperature.

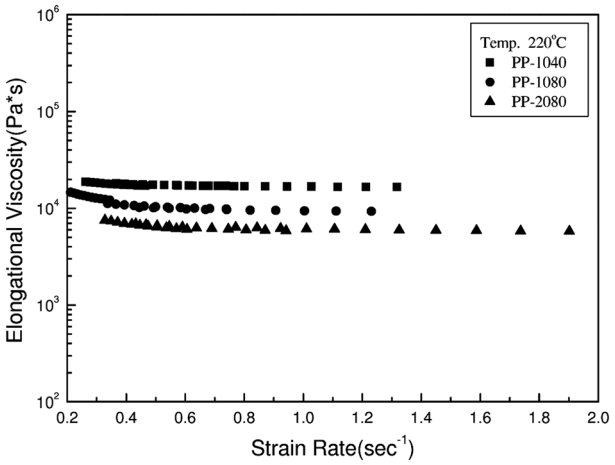

Figure 3. Elongation viscosity versus strain rate of PP-1040, PP-1080, and PP-2080 measured at 220°C.

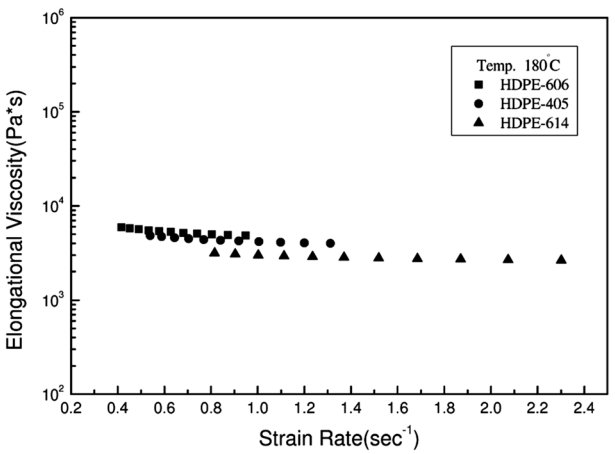

Figure 4. Elongation viscosity versus strain rate of HDPE-606, HDPE-405, and HDPE-614 measured at 180°C.

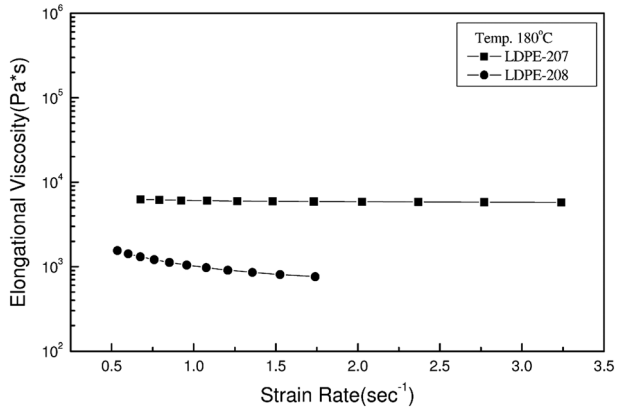

Figure 5. Elongation viscosity versus strain rate of LDPE-207 and LDPE-208 measured at 180°C.

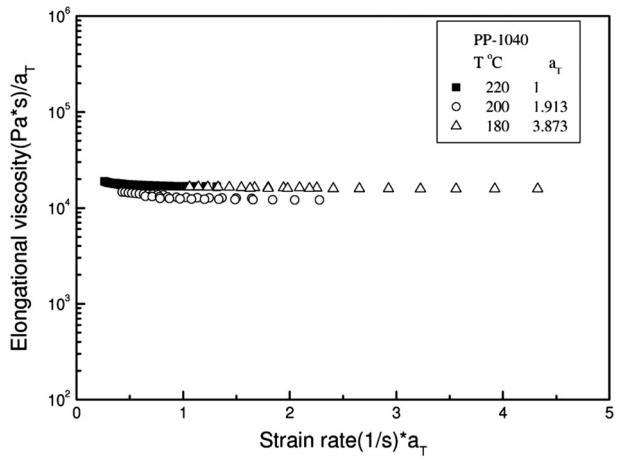

Figure 6. Master curve of elongation viscosity for PP-1040 with the reference temperature at 220°C.

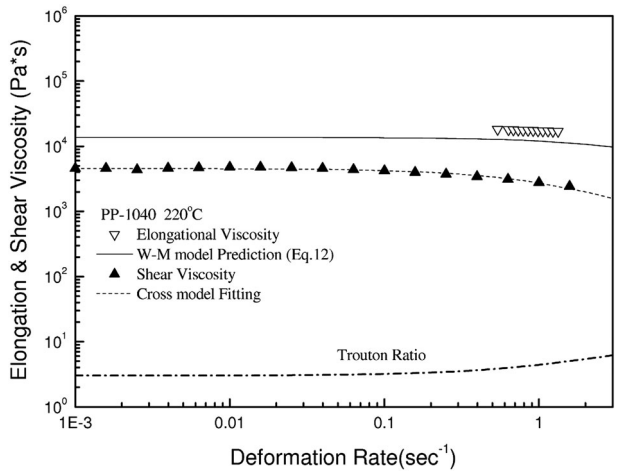

Figure 7. Elongation and shear viscosities, and the Trouton ratio at low deformation rates of PP-1040 at 220°C.

Comparison of experimental η_e with predictions derived from the W–M model

The experimental η_e of PP-1040 and HDPE-606, measured isothermally at 220°C and 180°C, are shown in Figs 7, 8, respectively,

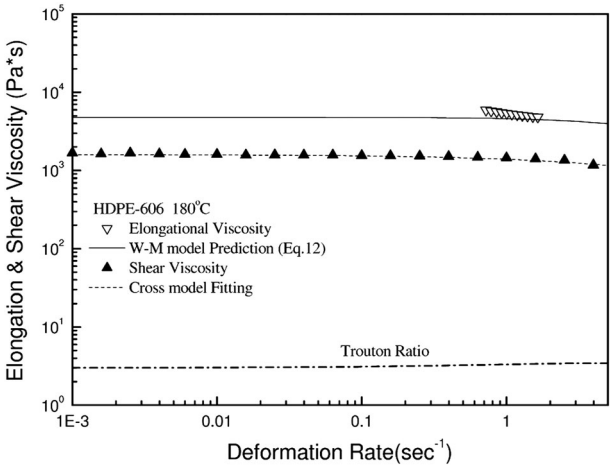

Figure 8. Elongation and shear viscosities, and the Trouton ratio at low deformation rates of HDPE-606 at 180°C.

along with the predictions of the W–M model. It should be noted that the deformation–rate ranges of these figures are so conformable to the scope of the linear relationship between the squared shear stress and the first normal stress difference as demonstrated in Fig. 1, that the shear modulus (G) in the W–M model could be reasonably obtained. The experimental η_S and the corresponding fitting curves by the Cross model are also shown for comparison. The experimental and the theoretical results were extremely similar; in particular, the measured elongation viscosity, irrespective of either PP or HDPE, was in good agreement with the predictions of the W–M model within the achievable range of strain rates. In addition, the Trouton ratio (T_R), defined as the ratio of η_e to η_S at the same strain rate, was plotted for PP-1040 and HDPE-606 in Figs 7, 8. For Newtonian liquids, the T_R value is 3 and the elastic liquids are noted for having high Trouton ratios. Any departure from the value 3 can be associated unambiguously with the viscoelasticity of the sample fluid. At extremely low strain rates, the T_R of both HDPE and PP approached 3 in the same manner, as expected. However, the T_R of PP increased with the increasing strain rate from approximately 0.1 s^{-1}, while for HDPE the T_R value nearly remained at 3 until the strain rate was 5 s^{-1}. It means that PP-1040 is more elastic than does HDPE-606 at high deformation rates. This can be attributed to the fact that both the molecular weight and its distribution, the polydispersity, of PP-1040 were greater than that of HDPE-606, as shown in Table 1.

Calculation of η_e using shear viscosity combined with the W–M model

Taking advantage of the measured shear viscosity along with the correlated material parameters of the W–M model, it is convenient to estimate the η_e using eqn (15). The results were illustrated in Figs. 9, 10, in which the shear viscosity measured using various rheometers was also shown for comparison together with the fitted η_S curve for PP-1040 and HDPE-606, respectively. The experimental η_e obtained in this work was able to fit the predicted curve of W–M model favorably, and a reasonable T_R as a function of deformation rates was also obtained; these results are much consistent with that of Barnes *et al.*[29] In addition, the T_R value of PP-1040 began to increase from the deformation rate of 0.1 s^{-1}, which was agreeable with the trend demonstrated in Fig. 7. However, the T_R value of HDPE-606

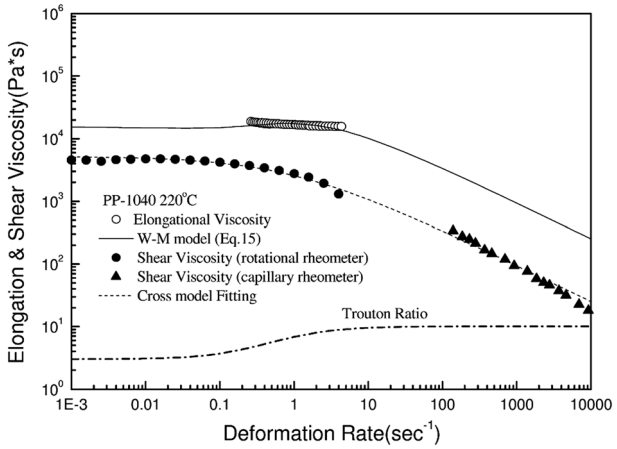

Figure 9. Elongation and shear viscosities, and the Trouton ratio as functions of deformation rates of PP-1040 at 220°C.

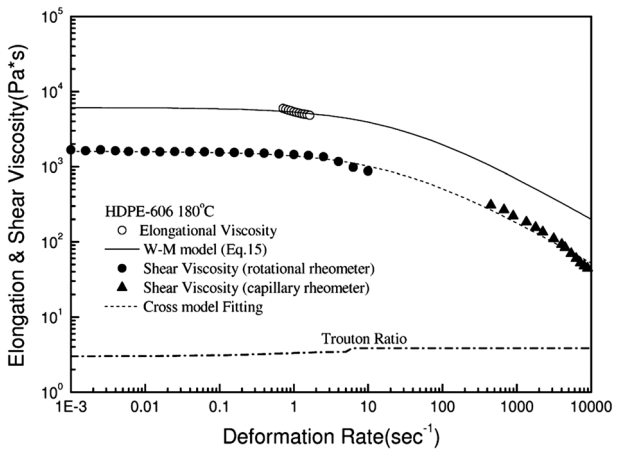

Figure 10. Elongation and shear viscosities, and the Trouton ratio as functions of deformation rates of HDPE-606 at 180°C.

remained nearly at a constant value within the entire range of strain rates, as shown in Figs 8 and 10. It can be attributed to the greater MW and MWD of PP-1040 relative to HDPE-606, leading to high elasticity of PP-1040 at high deformation rates.

CONCLUSIONS

The apparent elongation viscosity (η_e) of several molten polyolefins was measured using the isothermal fiber-spinning method. The White–Metzner (W–M) rheological model was used to predict the η_e as a function of the elongation strain rate, ranging from 0 to approximately $5\,s^{-1}$, in which the required material parameters were obtained by curve fitting the experimental data obtained from the shear measurements. The result of the comparison between the experimental data and the theoretical predictions was extremely successful at low strain rates. In addition, η_e could also be estimated directly from the measured shear viscosity (η_S) with a formulation using the W–M model; the subsequently obtained elongation viscosity and Trouton ratio (T_R) were reasonable within a wide range of strain rates. Based on the experimental and theoretical results, the polyolefin with a high molecular weight was observed to have high elongation viscosity, and the polymer with a broad molecular weight distribution also possessed high η_e. The T_R value of the commercial polypropylene (PP-1040) began to increase from 3 at a deformation rate of $0.1\,s^{-1}$ and grew up asymptotically to 10, whereas the T_R of HDPE-606 remained nearly at 3 within the entire range of strain rates. It means that PP-1040 is more elastic than does HDPE-606 at high deformation rates, which can be attributed to the greater MW and MWD of PP-1040 relative to HDPE-606. This corresponds with the application of the commercial PP-1040 as an yarn-grade extruded material to manufacture products such as heavy-duty woven bags, rope, and string; therefore, a high melt strength and elongation viscosity, thus high T_R value, is expected.

NOMENCLATURE

a	softening number (material constant in eqn (3))
a_T	temperature shifting factor
II_d	second invariant of tensor
d	rate of deformation tensor
G	shear modulus
$\underset{\approx}{I}$	unit tensor
MI	flow melt index
$\overline{M}n$	number average molecular weight
$\overline{M}w$	weight average molecular weight
MWD	molecular weight distribution
N_1	first normal stress difference
tr	Trace of a tensor (in eqn (3))
T_R	Trouton ratio

Greek Symbols

∇	gradient of a vector
$\dot{\gamma}$	shear strain rate
$\dot{\varepsilon}$	elongation strain rate
η_0	zero-shear-rate viscosity
η_e	elongation viscosity
η_S	shear viscosity
λ	relaxation time
σ	total stress tensor
τ	extra stress tensor

Superscripts

T	transpose of a matrix

Subscripts

0	at zero-shear rate
e	elongation flow
s	shear flow
~	vector
≈	tensor

Acknowledgements

Financial support provided by the Ministry of Science and Technology of Taiwan was greatly appreciated.

REFERENCES

[1] P. J. Wang, H. E. Lai, SPE ANTEC **2007**, 2494.
[2] Y. J. Chang, C. K. Yu, H. S. Chiu, W. H. Yang, H. E. Lai, P. J. Wang, SPE ANTEC **2009**,253.

[3] R. L. Ballman, *Rheol Acta* **1965**, *4*, 137.
[4] J. Meissner, *Rheol Acta* **1969**, *8*, 78.
[5] J. Meissner, *Rheol Acta* **1971**, *10*, 230.
[6] H. M. Laun, H. Munstedt, *Rheol Acta* **1978**, *17*, 415.
[7] Y. Ide, J.L. White, *J Appl Polym Sci* **1978**, *22*, 1061.
[8] Y. Suetsugu, J. L. White, *J Appl Polym Sci* **1983**, *22*, 1481.
[9] H. Yamane, J. L. White, *Polym Eng Rev* **1982**, *2*, 167.
[10] T. Sridhar, V. Tirtaatmadja, D. A. Nguyen, R. K. Gupta, *J Non-Newt Fluid Mech* **1991**, *40*, 271.
[11] T. Sridhar, R. K. Gupta, *J Rheol* **1991**, *35*, 363.
[12] V. Tirtaatmadja, T. Sridhar, *J Rheol* **1993**, *37*, 1081.
[13] D. Acierno, J. N. Dalton, J. M. Rodriguez, J.L. White, *J Appl Polym Sci* **1971**, *15*, 2395.
[14] R. R. Lamonte, C. D. Han, *J Appl Polym Sci* **1972**, *16*, 3285.
[15] N. E. Hudson, J. Ferguson, P. Meckie, *Trans Soc Rheol* **1974**, *18*, 541.
[16] V. G. Banker, J. E. Spruiell, J. L. White, *J Appl Polym Sci* **1977**, *21*, 2125.
[17] R. K. Bayer, *Rheol Acta* **1979**, *18*, 25.
[18] W. Minoshima, J. L. White, J. E. Spruiell, *J Appl Polym Sci* **1980**, *25*, 287.
[19] P. Revenu, J. Guillet, C. Carrot, *J Rheol* **1993**, *37*, 1041.
[20] F. N. Cogswell, *Polym Eng Sci* **1972**, *12*, 64.
[21] F. N. Cogswell, *Appl Polym Symp* **1975**, *27*, 1.
[22] D. M. Binding, *J Non-Newt Fluid Mech* **1988**, *27*, 173.
[23] D. M. Binding , K. Walters, *J Non-Newt Fluid Mech* **1988**, *30*, 233.
[24] H. A. Barnes, J. F. Hutton, K. Walters, *An introduction to rheology* , Elsevier, Amsterdam, **1989**.
[25] J. L. White, *Principles of polymer engineering rheology* , Wiley, New York, **1990**.
[26] J. M. Dealy, K. F. Wissbrun, *Melt rheology and its role in plastics processing: theory and applications*, Chapman & Hall, London, **1995**.
[27] R. Fulchiron , V. Verney , G. Marin, *J Non-Newt Fluid Mech* **1993**, *48*, 49.
[28] J. M. Reimers , J. M. Dealy, *J Rheol* **1996**, *40*, 167.
[29] H. A. Barnes, G. P. Roberts, *J Non-Newt Fluid Mech* **1992**, *44*, 113.
[30] J. L. White, W. Minoshima, *Polym Eng Sci* **1981**, *21*, 1113.
[31] R. G. Larson, *Constitutive Equations for Polymer Melts and Solutions*, Butterworths, Boston, **1988**.
[32] G. G. Lin, Y. H. Song, T. Y. Shiu, H. D. Cheng, *Polym Eng Sci* **2013**, DOI:10.1002/pen.23788.
[33] G. G. Lin, H. H. Shih, P. C. Chai, S. J. Hsu, *Polym Eng Sci* **2002**, *42*, 2213.
[34] G. G. Lin, M. C. Hu, *Adv Polym Tech* **1997**, *16*, 199.
[35] J. L. White, Y. Ide, *J Appl Polym Sci* **1978**, *22*, 3057.

